THE JOURNAL OF BIOLOGICAL CHEMISTRY VOL. 281, NO. 43, pp. 32485–32495, October 27, 2006

Role of Amino Acid Side Chains in Region 17–31 of Parathyroid Hormone (PTH) in Binding to the PTH Receptor*[S]

Received for publication, June 28, 2006, and in revised form, August 9, 2006 Published, JBC Papers in Press, August 21, 2006, DOI 10.1074/jbc.M606179200

Thomas Dean[‡], Ashok Khatri[‡], Zhanna Potetinova[§], Gordon E. Willick[§], and Thomas J. Gardella[‡1]

From the [‡]Endocrine Unit, Massachusetts General Hospital, and Harvard Medical School, Boston, Massachusetts 02114 and the [§]Institute for Biological Sciences, National Research Council, Ottawa, Ontario K1A 0R6, Canada

The principal receptor-binding domain (Ser^{17}–Val^{31}) of parathyroid hormone (PTH) is predicted to form an amphiphilic α-helix and to interact primarily with the N-terminal extracellular domain (N domain) of the PTH receptor (PTHR). We explored these hypotheses by introducing a variety of substitutions in region 17–31 of PTH-(1–31) and assessing, via competition assays, their effects on binding to the wild-type PTHR and to PTHR-delNt, which lacks most of the N domain. Substitutions at Arg^{20} reduced affinity for the intact PTHR by 200-fold or more, but altered affinity for PTHR-delNt by 4-fold or less. Similar effects were observed for Glu substitutions at Trp^{23}, Leu^{24}, and Leu^{28}, which together form the hydrophobic face of the predicted amphiphilic α-helix. Glu substitutions at Arg^{25}, Lys^{26}, and Lys^{27} (which forms the hydrophilic face of the helix) caused 4–10-fold reductions in affinity for both receptors. Thus, the side chains of Arg^{20}, together with those composing the hydrophobic face of the ligand's putative amphiphilic α-helix, contribute strongly to PTHR-binding affinity by interacting specifically with the N domain of the receptor. The side chains projecting from the opposite helical face contribute weakly to binding affinity by different mechanisms, possibly involving interactions with the extracellular loop/transmembrane domain region of the receptor. The data help define the roles that side chains in the binding domain of PTH play in the PTH-PTHR interaction process and provide new clues for understanding the overall topology of the bimolecular complex.

Parathyroid hormone (PTH)[2] plays a key role in calcium and phosphate homeostasis and has potent effects on the bone-remodeling process. PTH interacts with a Class 2 G protein-coupled receptor that is prominently expressed in bone osteoblasts and in cells located in the proximal and distal portions of the renal convoluted tubules. The PTH receptor (PTHR) is also expressed in the primordia of developing long bones, heart, mammary glands, and other tissues, where it mediates the morphogenic actions of PTH-related protein (PTHrP) (1).

For both PTH and PTHrP, the bioactive portions of the molecule reside within the first 34 amino acids of the processed polypeptides. Within region 1–34, the principal determinants of receptor-binding affinity and receptor-signaling activity map to the C- and N-terminal domains, respectively (2, 3). Solution-phase NMR studies of PTH-(1–34)-based ligands typically show a well formed α-helix in the region of the C-terminal binding domain (4, 5). This C-terminal α-helix, extending approximately from Ser^{17} to Val^{31} (5), exhibits strong amphiphilic character (6–8). PTH analog substitution studies have shown that the side chains of Trp^{23}, Leu^{24}, and Leu^{28}, which form the hydrophobic face of this α-helix, are particularly important for efficient interaction with the receptor (9–11).

The mechanism by which PTH interacts with its receptor has been investigated via the approaches of ligand analog design, receptor mutagenesis, and photochemical cross-linking (reviewed in Ref. 12). The view that has emerged from these studies is that the overall mechanism consists of two principal and, to some extent, autonomous components: 1) an interaction between the C-terminal helical domain of the ligand and the N-terminal extracellular domain (N domain; spanning Tyr^{23} to approximately Ile^{190}) of the mature receptor and 2) an interaction between the N-terminal portion of the ligand and the juxtamembrane domain (J domain) of the receptor containing the extracellular loops and seven transmembrane helices. The N domain component of the interaction is thought to provide the major portion of binding energy and stability to the complex, and the J domain component is thought to mediate the conformational changes involved in receptor activation (13). It now seems likely that most, if not all, of the 15 or so other Class 2 G protein-coupled receptors utilize a similar two-site binding mechanism for interacting with their cognate peptide ligands (14–16).

Consistent with such a two-site binding mechanism for PTH and the PTHR, we have shown that N-terminal PTH peptide fragments, such as PTH-(1–14), bind only extremely weakly to the receptor, but can nevertheless induce at least measurable increases in cAMP levels in PTHR-expressing cells (17). The potency of such N-terminal PTH fragments can be significantly enhanced by introducing substitutions that improve the affinity

* This work was supported in part by National Institutes of Health Grant DK-11794 (to T. J. G.). The costs of publication of this article were defrayed in part by the payment of page charges. This article must therefore be hereby marked "*advertisement*" in accordance with 18 U.S.C. Section 1734 solely to indicate this fact.

[S] The on-line version of this article (available at http://www.jbc.org) contains supplemental Figs. 1–3.

[1] To whom correspondence should be addressed: Endocrine Unit, Massachusetts General Hospital, Wellman Bldg., Rm. 503C, 50 Blossom St., Boston, MA 02114. Tel.: 617-726-3966; Fax: 617-726-7543; E-mail: gardella@helix.mgh.harvard.edu.

[2] The abbreviations used are: PTH, parathyroid hormone; PTHR, parathyroid hormone receptor; PTHrP, parathyroid hormone-related protein; N domain, N-terminal extracellular domain; J domain, juxtamembrane domain; IP, inositol phosphate; Aib, α-aminoisobutyric acid; Har, homoarginine; Bpa, *para*-benzoyl-L-phenylalanine; Bp, benzophenone; Cha, cyclohexylalanine; HPLC, high pressure liquid chromatography; Nle, norleucine; rPTH, rat parathyroid hormone; PipGly, (*S*)-4-piperidyl-*N*-amidino)glycine; Apa, (*S*)-2-amino-4-((2-amino)pyrimidinyl)butanoic acid; Gph, L-(4-guanidino)phenylalanine.

of the ligand for the PTHR J domain (18–20). Thus, the analog [$Aib^{1,3}$,Gln^{10},Har^{11},Trp^{14}]PTH-(1–14)-NH_2 is equipotent to PTH-(1–34) in stimulating cAMP as well as inositol phosphate (IP) production in PTHR-expressing cells. Moreover, such optimized N-terminal PTH analogs retain full potency in cells expressing PTHR-delNt, a PTHR construct that lacks most (Ala^{24}–Arg^{181}) of the N domain, whereas unmodified PTH-(1–34) exhibits at least 100-fold reductions in potency and affinity for PTHR-delNt compared with its actions on the intact PTHR (18–20).

The large reduction in affinity/potency that unmodified PTH-(1–34) exhibits for PTHR-delNt can be attributed, according to the two-site interaction model, to the loss of the binding interactions that normally occur between the C-terminal helical domain of the ligand and the N domain of the receptor. The cross-linking approach has indeed established spatial proximities between PTH residues 23, 27, and 28, when substituted with *para*-benzoyl-L-phenylalanine (Bpa), and the N domain of the receptor (21, 22). On the other hand, [$Lys^{27}(Bp)_2$]PTH-(1–34)-NH_2, which contains the photoreactive Bp moiety attached to the Lys^{27} side chain amino groups, was shown to cross-link to the first extracellular loop of the PTHR (23). This observation raised the possibility that the C-terminal binding domain of PTH can functionally interact with the receptor J domain. Consistent with this possibility, we recently showed that methylation of several backbone nitrogen atoms in region 17–31 of PTH-(1–31) impairs, albeit modestly, the capacity of the ligand to stimulate cAMP formation in cells expressing PTHR-delNt (8). Taken together, these observations point to the uncertainty that exists in our understanding of the specific mechanisms by which the C-terminal domain of PTH contributes to the PTHR-binding process.

This study was undertaken to examine further the mode of action used by the C-terminal binding domain of PTH. We sought to address the roles that the side chains in this domain play in the PTHR-binding process, the general functional importance of amphiphilicity, and the potential for binding interactions with the receptor J domain. Our strategy was to introduce a variety of conservative and non-conservative substitutions in region 17–31 of PTH-(1–31)-NH_2 and to assess their effects on binding to the intact PTHR and to PTHR-delNt. The overall results indicate a dominant role for specific interactions between side chains on the hydrophobic face of the C-terminal helix and the receptor N-terminal domain. They also provide evidence for weak interactions between side chains projecting from the hydrophilic face of the helix and the PTHR J domain. The data also shed new light on the overall topology of the bimolecular complex, as they support folding of the bound ligand and proximity of the binding sites in the N and J domains of the receptor.

MATERIALS AND METHODS

Peptide Synthesis—Peptides were based on the human PTH-(1–31)-NH_2 sequence (SVSEIQLMHNLGKHLNSMERVEW-LRKKLQDV-NH_2). The alanine substitutions were incorporated into this otherwise unmodified PTH-(1–31)-NH_2 scaffold. Subsequently, cyclohexylalanine (Cha) and Glu substitutions were incorporated into the [Ala^1,Arg^{19}]PTH-(1–31)-NH_2 scaffold, which, because of the $Ser^1 \rightarrow Ala$ and $Glu^{19} \rightarrow Arg$ substitutions, exhibits improved affinity for PTHR-delNt (19, 24). These Ala-, Cha-, and Glu-substituted PTH-(1–31)-NH_2 and [Ala^1,Arg^{19}]PTH-(1–31)-NH_2 peptides and their corresponding parental controls were synthesized by the Massachusetts General Hospital Biopolymer Core facility using conventional methodologies as we described previously (20). Additional analogs of PTH-(1–31)-NH_2 with substitutions at position 20 were prepared as part of a previous study (25). All peptides were verified by analytical HPLC, matrix-assisted laser desorption ionization mass spectrometry, and amino acid analysis, and peptide concentrations of stock solutions were established by amino acid analysis. The radioligands ^{125}I-[$Nle^{8,21}$,Tyr^{34}]rPTH-(1–34)-NH_2 and ^{125}I-[$Aib^{1,3}$,Nle^8,Gln^{10},Har^{11},Ala^{12},Trp^{14},Tyr^{15}]rPTH-(1–15)-NH_2 (henceforth referred to as ^{125}I-[$Aib^{1,3}$,M]rPTH-(1–15)-NH_2) were prepared by the oxidative chloramine-T procedure using $Na^{125}I$ (specific activity of 2200 Ci/mmol; PerkinElmer Life Sciences) and purified by reversed-phase HPLC.

Circular Dichroism—CD spectra were obtained on a Jasco J-600 spectropolarimeter at 20 °C. Four spectra were averaged, and the data were smoothed by the Jasco software. The instrument was calibrated with ammonium (+)-10-camphorsulfonate. Data are expressed as the number of helical residues/peptide chain as calculated from $-[\theta]_{222} \times 30/28{,}000$, where $[\theta]_{222}$ is the mean residue ellipticity at 222 nm, as we described previously (8).

Cell Culture—Cells were cultured at 37 °C in a humidified atmosphere containing 5% CO_2 in Dulbecco's modified Eagle's medium supplemented with 10% fetal bovine serum (HyClone, Logan UT), 100 units/ml penicillin G, and 100 μg/ml streptomycin sulfate (Invitrogen). For binding and cAMP experiments performed with the intact PTHR, the HKRK-B7 and ROS 17/2.8 cell lines were used. HKRK-B7 cells are derived from the porcine kidney cell line LLC-PK_1 and express, via stable DNA transfection, the wild-type human PTHR at an approximate surface density of 950,000 PTH-binding sites/cell (26). ROS 17/2.8 cells are rat osteosarcoma cells and express the endogenous PTHR at an approximate surface density of 70,000 PTH-binding sites/cell (27). The cells were plated and assayed in 24-well plates.

PTHR-delNt was derived from the human PTHR by site-directed mutagenesis and lacks most (Ala^{24}–Arg^{181}) of the N domain (28). PTHR-delNt was expressed in COS-7 cells via transient DNA transfection. For binding assays, cell membranes were prepared from the transfected COS-7 cells. To increase the maximum binding of ^{125}I-[$Aib^{1,3}$,M]rPTH-(1–15)-NH_2 to PTHR-delNt in these membranes, the cells were cotransfected with a negative-dominant mutant $G\alpha_s$ protein ($G\alpha_s(\alpha_3\beta_5/Gly^{226} \rightarrow Ala/Ala^{366} \rightarrow Ser)$; hereafter referred to as $G\alpha_s^{ND}$). This mutant $G\alpha_s$ subunit is thought to couple to cognate receptors, and thus stabilize high affinity receptor conformations more efficiently than does wild-type $G\alpha_s$ without increasing basal cAMP levels (29). We recently used a precursor of this $G\alpha_s$ mutant, $G\alpha_s(\alpha_3\beta_5)$, to increase the binding of ^{125}I-[$Aib^{1,3}$,M]rPTH-(1–15)-NH_2 to PTHR-delNt in COS-7 cell membranes (18). We subsequently found that $G\alpha_s^{ND}$, which contains the same five-amino acid replacement of the corre-

sponding $G\alpha_i$ residues in the $\alpha_3\beta_5$ loop as does $G\alpha_s(\alpha_3\beta_5)$ plus the point mutations $Gly^{226} \rightarrow Ala$, which increases affinity for $G\beta/\gamma$, and $Ala^{366} \rightarrow Ser$, which decreases affinity for GDP (29), yielded ~2-fold higher levels of specific binding of ^{125}I-[$Aib^{1,3}$,M]rPTH-(1–15)-NH_2 than did $G\alpha_s(\alpha_3\beta_5)$ (data not shown). The COS-7 cells were cotransfected in 6-well plates using plasmid DNA encoding PTHR-delNt (1 μg/well), plasmid DNA encoding $G\alpha_s^{ND}$ (1 μg/well), and FuGENE 6 reagent (6 μl/well; Roche Diagnostics). Control experiments were performed with COS-7 cells similarly cotransfected with $G\alpha_s^{ND}$ and the wild-type PTHR. Cells were harvested 3 days after transfection, and membranes were prepared as described (18).

Receptor Binding—Binding to the intact PTHR in HKRK-B7 and ROS 17/2.8 cells was assessed using ^{125}I-[$Nle^{8,21}$, Tyr^{34}]rPTH-(1–34)-NH_2 as a tracer radioligand as described (28). In brief, confluent cells in 24-well plates (~500,000 cells/well) were incubated in binding buffer (50 mM Tris-HCl, 100 mM NaCl, 5 mM KCl, 2 mM $CaCl_2$, 5% heat-inactivated horse serum, 0.5% fetal bovine serum, adjusted to pH 7.7 with HCl) containing radioligand (~100,000 cpm/well) with or without unlabeled peptide ligand (3×10^{-9} to 1×10^{-5} M) for 4 h at 15 °C. The binding mixture was then removed by aspiration' the cells were rinsed three times with binding buffer and lysed in 1 M NaOH; and the entire lysate was counted for γ-irradiation in a γ-counter. Binding to PTHR-delNt in COS-7 cell membranes was assessed in 96-well vacuum filtration plates (MultiScreen-HV Durapore, 0.65-μm membranes; Millipore Corp.) using ^{125}I-[$Aib^{1,3}$,M]rPTH-(1–15)-NH_2 as a tracer radioligand as described (18). In brief, cell membranes (20 μg/well) were incubated in membrane binding buffer containing radioligand (~30,000 cpm/well) with or without unlabeled peptide ligand (3×10^{-9} to 1×10^{-5} M) for 90 min at 21 °C (reaction volume of 200 μl). The plates were then subjected to rapid vacuum filtration, and the filters were washed once with buffer, air-dried, detached from the plate, and counted for γ-irradiation in a γ-counter. Nonspecific binding was defined as the binding observed in the presence of 1×10^{-6} M PTH-(1–31)-NH_2 for HKRK-B7 and ROS 17/2.8 cells and of 1×10^{-6} M [$Aib^{1,3}$,M]rPTH-(1–15)-NH_2 for PTHR-delNt. Specifically bound radioactivity was calculated as a percentage of the radioactivity specifically bound in the absence of competing ligand.

Stimulation of Intracellular cAMP and IP—The capacities of the ligands to stimulate formation of cAMP were assessed in intact ROS 17/2.8 cells, as described (28). In brief, cells in 24-well plates were incubated in binding buffer containing the phosphodiesterase inhibitor 3-isobutyl-1-methylxanthine (2 mM) with or without a peptide ligand (3×10^{-11} to 1×10^{-6} M) for 30 min at room temperature. The medium was then removed, and the cells were lysed by adding 50 mM HCl and freezing the plate on dry ice. The cAMP in the thawed lysate was quantified by radioimmunoassay. The stimulation of production of inositol phosphates ($IP_1 + IP_2 + IP_3$) was assessed in COS-7 cells transfected with the intact human PTHR as we described previously (28). In brief, intact transfected COS-7 cells in 24-well plates were labeled with *myo*-[^{3}H]inositol (specific activity of 25 Ci/mmol; PerkinElmer Life Sciences) for 16 h. The labeled cells were then treated for 30 min with ligand in the presence of $LiCl_2$ (30 mM), and the medium was removed and replaced with ice-cold trichloroacetic acid (5%). After 2 h on ice, the acid lysates were extracted with ether and processed by ion-exchange chromatography (0.5-ml resin bed), and the ammonium formate-eluted [^{3}H]inositol phosphates were quantified by liquid scintillation counting.

Data and Statistical Calculations—Binding and cAMP data were processed for curve fitting and derivation of IC_{50} and EC_{50} values using least-squares nonlinear regression analysis and the following equation: $y = y_{min} + (y_{max} - y_{min})/1 + (IC_{50}/x)^n$, where y, y_{min}, and y_{max} are the observed, minimum, and maximum response values, respectively; x is the ligand concentration; and n is the slope factor. In cases in which incomplete inhibition of binding occurred, *e.g.* with certain PTH-(1–31)-NH_2 analogs binding to PTHR-delNt, the curves were extrapolated to nonspecific binding. Paired data sets were statistically compared using a two-tailed Student's t test, assuming unequal variance for the two sets.

RESULTS

Alanine Scan of Region 17–31 of PTH—We first individually replaced each residue in region 17–31 of PTH-(1–31)-NH_2 with alanine and assessed the effects of the substitutions on binding to the intact human PTHR stably expressed in HKRK-B7 cells. Binding was assessed by competition methods using ^{125}I-[$Nle^{8,21}$,Tyr^{34}]rPTH-(1–34)-NH_2 as a tracer radioligand. The parental PTH-(1–31)-NH_2 peptide fully inhibited the binding of this tracer with an IC_{50} of 68 ± 10 nM (Fig. 1*A* and Table 1). The various alanine substitutions had a range of effects on this binding. Most dramatic was that of the $Arg^{20} \rightarrow$ Ala substitution, which abolished detectable binding (Fig. 1*A*). The alanine substitutions at Trp^{23} and Leu^{24} reduced the apparent binding affinity by 19- and 12-fold, respectively, relative to the parental peptide ($p < 0.05$). The alanine substitutions at Val^{21}, Arg^{25}, Lys^{27}, Leu^{28}, and Val^{31} reduced affinity by ~3-fold, and the remaining alanine substitutions altered affinity by 2-fold or less (Fig. 1, *A* and *B*; and Table 1). The alanine substitutions at Glu^{19}, Glu^{22}, and Gln^{29} each produced a small (≤2-fold) enhancement of the apparent binding affinity, as did the $Glu^{19} \rightarrow$ Arg substitution, which we have shown previously to enhance cAMP-stimulating potency in PTH-(1–34) and PTH-(1–20) peptides (24). The Ala^{22} substitution was thus paired with Ala^{19} as well as with Arg^{19}, but neither pairing improved affinity further relative to the single substitutions alone (Table 1).

We then assessed the effects of the alanine substitutions on binding to PTHR-delNt. For these experiments, we used membranes prepared from COS-7 cells transiently transfected with PTHR-delNt. As a tracer radioligand, we used ^{125}I-[$Aib^{1,3}$,M]rPTH-(1–15)-NH_2, which we have shown binds exclusively to the PTHR J domain (30). To increase the total specific binding of ^{125}I-[$Aib^{1,3}$,M]rPTH-(1–15)-NH_2 to these membranes, the cells were cotransfected with a negative-dominant mutant $G\alpha_s$ subunit ($G\alpha_s^{ND}$), which promotes ligand binding presumably by stabilizing high affinity receptor conformations (29).

Unlabeled [$Aib^{1,3}$,M]rPTH-(1–15)-NH_2 (used as a control peptide) fully inhibited the binding of ^{125}I-[$Aib^{1,3}$,M]rPTH-(1–15)-NH_2 to these membranes with high apparent affinity

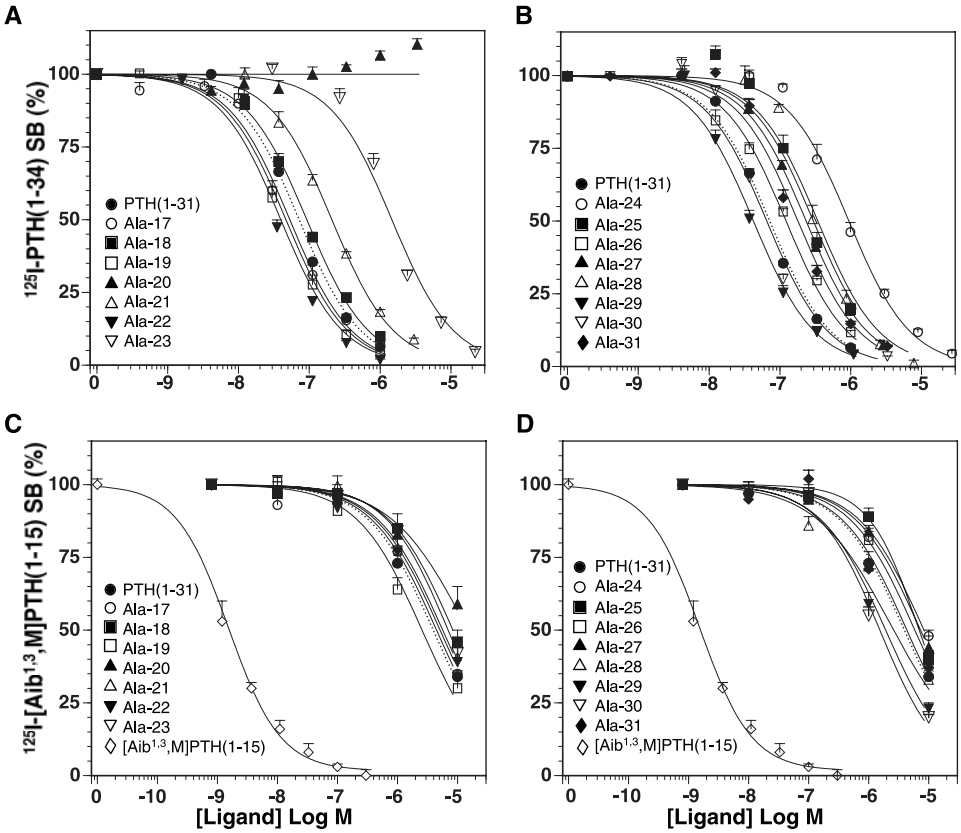

FIGURE 1. **Alanine scan of region 17–31 of PTH-(1–31)-NH$_2$.** PTH-(1–31)-NH$_2$ and analogs thereof with individual alanine substitutions in region 17–31 were assessed by competition methods for binding to the intact PTHR (*A* and *B*) and to PTHR-delNt (*C* and *D*). Intact HKRK-B7 cells stably transfected with the PTHR and the ^{125}I-[Nle^{8,21},Tyr^{34}]rPTH-(1–34)-NH$_2$ (*^{125}I-PTH(1–34)*) tracer radioligand were used in the assays in *A* and *B*; membranes prepared from COS-7 cells transiently transfected with PTHR-delNt and the ^{125}I-[Aib^{1,3},M]rPTH-(1–15)-NH$_2$ tracer radioligand were used in *C* and *D*. To increase the total binding of ^{125}I-[Aib^{1,3},M]rPTH-(1–15)-NH$_2$, the COS-7 cells were cotransfected with a negative-dominant Gα_s mutant. For the experiments with PTHR-delNt, unlabeled [Aib^{1,3},M]rPTH-(1–15)-NH$_2$ (◇) was used as a control and to determine nonspecific binding, to which the curves for the PTH-(1–31) analogs were extrapolated. Data for the parental PTH-(1–31) peptide (● and *dotted line*) are shown in each panel. Data are the means ± S.E. of three or more experiments, each performed in duplicate. *SB*, specific binding.

(IC_{50} = 2.2 ± 0.5 nM) (Fig. 1, *C* and *D*; and Table 1). As expected from the absence of ligand interactions with the PTHR N domain, unmodified PTH-(1–31)-NH$_2$ bound to PTHR-delNt with relatively low affinity (IC_{50} = 3700 ± 400 nM) (Fig. 1, *C* and *D*; and Table 1). This binding was nevertheless sufficient to assess the effects of the alanine substitutions on the capacity of the ligand to interact with PTHR-delNt. None of the alanine substitutions altered binding to PTHR-delNt by >5-fold, including the Arg^{20} → Ala substitution, which had strongly diminished binding to the intact PTHR (Fig. 1, *A versus C*). Similarly, the Ala substitutions at Trp^{23} and Leu^{24}, which reduced affinity for the PTHR by 19- and 12-fold, respectively, reduced affinity for PTHR-delNt by only ~2-fold. These findings indicate that the mechanisms by which the Ala substitutions at Arg^{20}, Trp^{23}, and Leu^{24} impair binding to the intact PTHR are largely independent of interactions with the PTHR J domain.

None of the alanine substitutions had a major impact on the secondary structure of the peptide as revealed by CD spectroscopy analysis. Thus, the CD spectrum of each analog exhibited clear negative deflections in the regions at 209 and 222 nm, which are indicative of α-helical structure (Fig. 2). The number of helical resides/peptide chain (calculated from the CD signal at 222 nm) was between 7 and 10 for each peptide (Table 1). These findings are consistent with a preservation of α-helical structure in region 17–31 of the ligand (6, 8) as well as with the known helix-forming propensity of alanine (31).

Substitutions with Cha—The strong effects that the alanine substitutions at Trp^{23}, Leu^{24}, and Leu^{28} had on binding to the intact PTHR (Fig. 1, *A* and *B*) suggested that hydrophobicity *per se* in region 17–31 of PTH might play a key role in determining the affinity of ligand for the receptor. To evaluate this further, we substituted each residue in region 17–31 of PTH with Cha, an amino acid analog that would preserve bulk hydrophobicity, yet alter the specific chemistry and topology of the side chain at the substituted site. We used [Ala^1,Arg^{19}]PTH-(1–31)-NH$_2$ as a scaffold peptide in these experiments, as we wanted to augment our capacity to assess binding to PTHR-delNt, and the Glu^{19} → Arg and Ser^1 → Ala substitutions were known to improve interaction with this truncated receptor (19, 24).

The effects of the Cha substitutions on the intact PTHR in HKRK-B7 cells generally paralleled those of the corresponding alanine substitutions. Thus, relative to the parental [Ala^1,Arg^{19}]PTH-(1–31)-NH$_2$ peptide, the Cha substitution at Arg^{20} had the strongest effect on binding and reduced affinity by 120-fold (p = 0.005). Substitutions at Trp^{23} and Leu^{24} reduced affinity by 14- and 11-fold, respectively (p < 0.002), and those at the remaining positions altered PTHR-binding affinity by 6-fold or less (Fig. 3, *A* and *B*; and Table 2). The deleterious effects that the Cha substitutions at Trp^{23} and Leu^{24} had on PTHR-binding affinity indicate that hydrophobicity *per se* is not the main physicochemical property of these two side chains that underlies their contributions to PTHR-binding affinity.

CD analyses again indicated that none of the Cha substitutions disrupted the α-helical content of the peptide (Table 2 and supplemental Fig. 1*B*). The Cha^{20}- and Cha^{27}-substituted analogs exhibited enhanced negative deflections at 209 and 222 nm, which resulted in calculated helical content values that were ~2-fold higher than that of the parental peptide. The basis for these enhanced CD signals (which were not accompanied by parallel changes in our receptor assays) is not clear at present.

The Cha substitutions at Arg^{25} and Lys^{26} reduced affinity for PTHR-delNt by ~5–7-fold, and the remaining Cha substitu-

TABLE 1

Helical contents and PTHR-binding properties of PTH-(1–31)-NH_2 analogs

Substitutions were introduced into PTH-(1–31)-NH_2. The helical residue values were calculated from the mean residue ellipticity ($[\theta]_{222}$) observed in the CD spectra at 222 nm. Competition binding studies with the wild-type PTHR (PTHR-WT) were performed in intact HKRK-B7 cells using ^{125}I-[Nle^{8,21}, Tyr^{34}]rPTH-(1–34)-NH_2 as a tracer radioligand. Those with PTHR-delNt were performed in membranes prepared from COS-7 cells transiently transfected with PTHR-delNT and a negative-dominant $G\alpha_s$ mutant; ^{125}I-[Aib^{1,3},M]rPTH-(1–15)-NH_2 was used as a tracer radioligand, and unlabeled [Aib^{1,3},M]rPTH-(1–15)-NH_2 was used as a control. Binding IC_{50} values are the means ± S.E. of data from the number of experiments indicated in parentheses. Cit, citralline, Orn, ornithine; ND, not determined.

	CD helical residues	IC_{50}	
		PTHR-WT (HKRK-B7 cells)	PTHR-delNt (COS-7 cells)
		mM	*nM*
PTH-(1–31)-NH_2	8	68 ± 10 (23)	3666 ± 431 (13)
Ser^{17} → Ala	10	57 ± 12 (4)	4678 ± 386 (4)
Met^{18} → Ala	10	92 ± 14 (3)	8799 ± 2334 (4)
Glu^{19} → Ala	9	49 ± 11 (4)	2940 ± 833 (4)
Arg^{20} → Ala	10	>10,000 (3)	19,343 ± 8100 (4)
Val^{21} → Ala	10	200 ± 18 (3)	5686 ± 486 (4)
Glu^{22} → Ala	9	36 ± 2 (4)	5857 ± 2237 (4)
Trp^{23} → Ala	7	1312 ± 139 (3)	7357 ± 1832 (4)
Leu^{24} → Ala	7	807 ± 165 (3)	8764 ± 1167 (4)
Arg^{25} → Ala	7	281 ± 67 (3)	7177 ± 1083 (4)
Lys^{26} → Ala	7	125 ± 8 (3)	6210 ± 948 (4)
Lys^{27} → Ala	9	217 ± 7 (3)	7288 ± 615 (4)
Leu^{28} → Ala	8	290 ± 63 (3)	3459 ± 482 (4)
Gln^{29} → Ala	9	44 ± 11 (3)	1931 ± 303 (4)
Asp^{30} → Ala	10	63 ± 7 (4)	1545 ± 215 (4)
Val^{31} → Ala	9	176 ± 23 (4)	4911 ± 1341 (4)
Glu^{19} → Ala/Glu^{22} → Ala	9	49 ± 9 (4)	619 ± 75 (4)
Glu^{19} → Arg/Glu^{22} → Arg	8	54 ± 13 (4)	360 ± 19 (4)
Glu^{19} → Arg	8	42 ± 6 (4)	1226 ± 332 (4)
Arg^{20} → Gln	7	>10,000 (3)	10,284 ± 121 (3)
Arg^{20} → Glu	7	>10,000 (3)	14,747 ± 324 (3)
Arg^{20} → Lys	8	>10,000 (3)	7105 ± 1275 (3)
Arg^{20} → Nle	12	15,404 ± 2334 (4)	10,688 ± 1033 (3)
Arg^{20} → Cit	9	11,925 ± 2151 (4)	10,624 ± 1612 (3)
Arg^{20} → Orn	6	>10,000 (4)	5530 ± 279 (3)
Arg^{20} → Apa	ND	>10,000 (3)	5740 ± 775 (3)
Arg^{20} → Gph	ND	>10,000 (3)	2047 ± 442 (3)
Arg^{20} → PipGly	8	14135 ± 5345 (4)	6605 ± 2407 (5)
[Aib^{1,3},M]rPTH-(1–15)-NH_2	ND	ND	2.2 ± 0.5 (8)

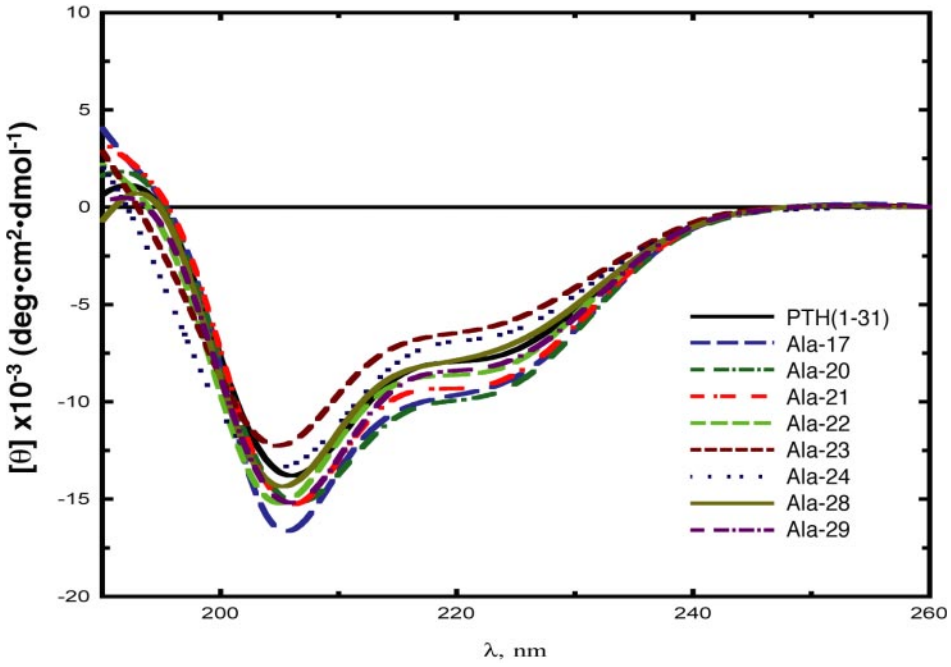

FIGURE 2. **CD spectroscopy of alanine-substituted PTH-(1–31)-NH_2 analogs.** The parental PTH-(1–31)-NH_2 peptide and derivatives thereof altered by a single alanine substitution in region 17–31 were analyzed by CD spectroscopy. The negative deflections in the mean residue ellipticity ($[\theta]$) in the regions at 209 and 222 nm of the spectra are indicative of α-helical structure. The CD spectra obtained for other peptides used in this study are shown in supplemental Fig. 1. For each peptide, the number of helical residues/peptide chain was calculated from $[\theta]_{222}$, and the resulting values are reported in Tables 1 and 2. *deg*, degrees.

tions, including those at Arg^{20}, Trp^{23}, and Leu^{24}, altered apparent affinity by 3-fold or less (Fig. 3, *C* and *D*; and Table 2). These results are in agreement with those obtained with the corresponding Ala substitutions in that they suggest that the detrimental effects that substitutions at positions 20, 23, and 24 have on binding to the intact PTHR are not due to altered interactions with the PTHR J domain, but rather involve interactions with the receptor N domain. They also suggest that Arg^{25} and Lys^{26} can contribute to PTHR-binding affinity via mechanisms that are not dependent on interactions with the receptor N domain.

Non-conservative Glu Substitutions—The data so far suggested that certain residues in the C-terminal domain of PTH-(1–31), especially Trp^{23}, Leu^{24}, and Leu^{28}, contribute significantly to PTHR-binding affinity by interacting predominantly with the receptor N domain. To test this hypothesis further, we sought to

introduce substitutions that would more strongly disrupt binding to the intact PTHR than did the alanine or Cha substitutions. If the hypothesis were correct, then such substitutions would have little or no effect on binding to PTHR-delNt. We therefore introduced, as a non-conservative substitution, Glu at each position in the C-terminal segment of [Ala^1,Arg^{19}]PTH-(1–31)-NH_2 that was otherwise occupied by a hydrophobic or positively charged amino acid. The analogs were again assessed for binding to the intact PTHR and to PTHR-delNt. As predicted, several of the Glu substitutions caused severe reductions in binding affinity for the intact PTHR. Thus, the Glu substitutions at Arg^{20} and Leu^{24} abolished detectable binding to the intact PTHR, and those at Leu^{28} and Trp^{23} reduced apparent affinity by 270- and 160-fold, respectively (Fig. 4, *A* and *B*; and Table 2). Modest 2–12-fold reductions in PTHR-binding affinity occurred with the Glu substitutions at Arg^{19}, Val^{21}, Arg^{25}, Lys^{26}, and Lys^{27}. None of the Glu substitutions substantially altered the CD profile of the peptide (Table 2 and supplemental Fig. 1*C*).

Each of the Glu substitutions had only a mild impact on binding to PTHR-delNt. Thus, Glu substitutions at Arg^{20}, Trp^{23}, Leu^{24}, and Leu^{28}, which severely reduced affinity for the PTHR, reduced affinity for the truncated PTHR by <3-fold (Fig. 4, *C* and *D*; and Table 2). The Glu substitutions at Val^{21} and Arg^{25}

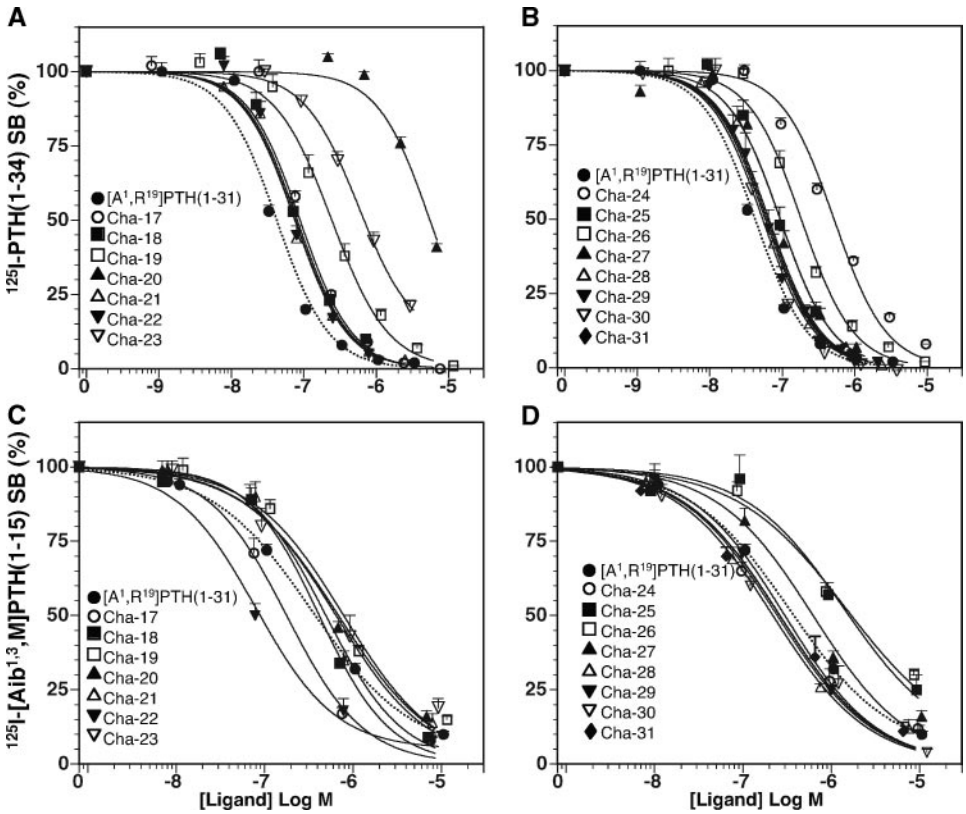

FIGURE 3. **Cha scan of region 17–31 of [Ala^1,Arg^{19}]PTH-(1–31)-NH_2.** Residues in region 17–31 of [Ala^1,Arg^{19}]PTH-(1–31)-NH_2 (*[A^1,R^1]PTH(1–31)*) were individually replaced with Cha, and the effects on binding to the intact PTHR (*A* and *B*) and to PTHR-delNt (*C* and *D*) were assessed as described in the legend to Fig. 1. Data are the means ± S.E. of three or more experiments, each performed in duplicate. *^{125}I-PTH(1–34) SB*, ^{125}I-[NIe^{8,21},Tyr^{34}]rPTH-(1–34)-NH_2-specific binding.

TABLE 2

Helical contents and PTHR-binding properties of [Ala^1, Arg^{19}]-PTH-(1–31)-NH_2 analogs

Cha and Glu substitutions were introduced into [Ala^1, Arg^{19}]PTH-(1–31)-NH_2. Data were obtained as described in the legend to Table 1. PTHR-WT, the wild-type PTHR.

	CD helical residues	IC_{50}	
		PTHR-WT (HKRK-B7 cells)	PTHR-delNt (COS-7 cells)
[Ala^1, Arg^{19}]PTH-(1–31)-NH_2	8	38 ± 8 (7)	397 ± 40 (4)
Ser^{17} → Cha	9	112 ± 13 (3)	179 ± 41 (4)
Met^{18} → Cha	8	87 ± 13 (3)	408 ± 32 (4)
Arg^{19} → Cha	10	233 ± 57 (3)	780 ± 83 (4)
Arg^{20} → Cha	16	4738 ± 333 (3)	632 ± 79 (4)
Val^{21} → Cha	9	74 ± 15 (3)	564 ± 172 (4)
Glu^{22} → Cha	8	75 ± 9 (3)	126 ± 45 (4)
Trp^{23} → Cha	8	546 ± 70 (3)	867 ± 402 (4)
Leu^{24} → Cha	9	436 ± 10 (3)	283 ± 68 (4)
Arg^{25} → Cha	9	103 ± 27 (3)	2711 ± 1306 (4)
Lys^{26} → Cha	6	172 ± 27 (3)	1872 ± 281 (4)
Lys^{27} → Cha	18	91 ± 17 (3)	629 ± 72 (4)
Leu^{28} → Cha	8	65 ± 10 (3)	226 ± 39 (4)
Gln^{29} → Cha	8	61 ± 14 (3)	319 ± 57 (4)
Asp^{30} → Cha	8	54 ± 7 (3)	305 ± 126 (4)
Val^{31} → Cha	9	66 ± 20 (3)	466 ± 298 (4)
Arg^{19} → Glu	9	125 ± 29 (4)	18,856 ± 9649 (5)
Arg^{20} → Glu	8	>10,000 (3)	776 ± 380 (5)
Val^{21} → Glu	7	447 ± 172 (4)	1615 ± 516 (5)
Trp^{23} → Glu	7	6044 ± 2636 (3)	434 ± 84 (5)
Leu^{24} → Glu	6	>10,000 (3)	1041 ± 197 (5)
Arg^{25} → Glu	5	189 ± 53 (4)	1629 ± 274 (5)
Lys^{26} → Glu	6	60 ± 19 (3)	832 ± 215 (5)
Lys^{27} → Glu	5	156 ± 50 (3)	1266 ± 293 (5)
Leu^{28} → Glu	5	10,360 ± 3983 (3)	974 ± 252 (5)

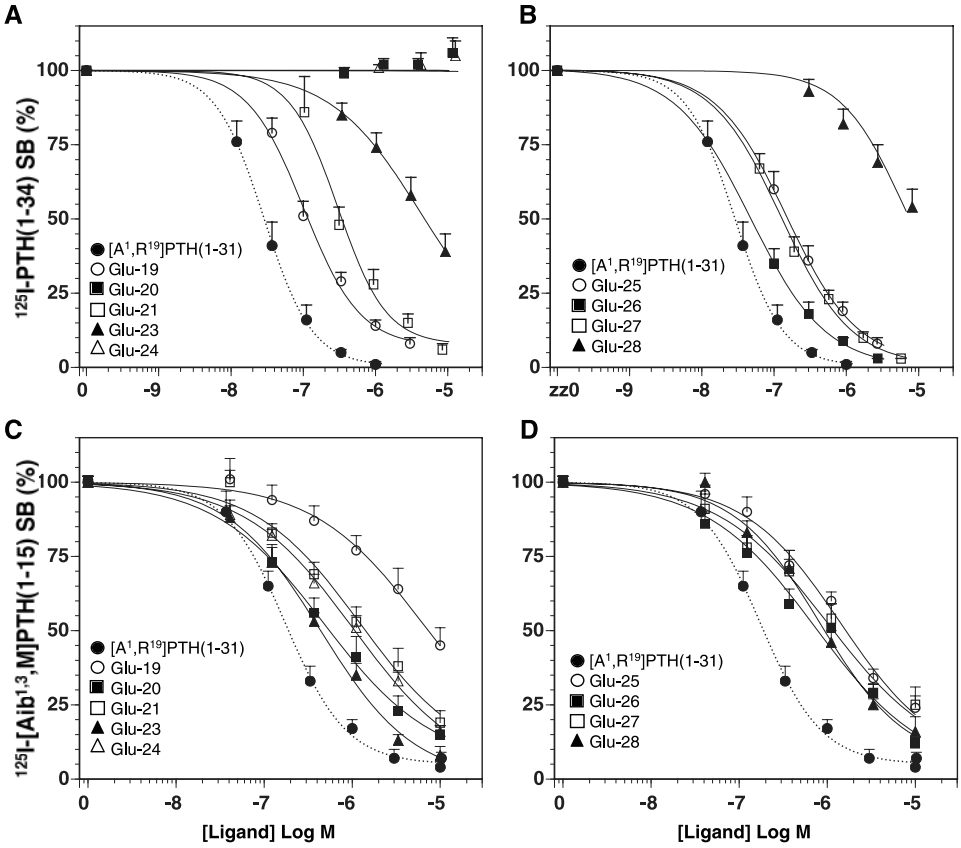

FIGURE 4. **Effects of Glu substitutions in region 19–28 of [Ala^1,Arg^{19}]PTH-(1–31)-NH$_2$.** Residues in region 19–28 of [Ala^1,Arg^{19}]PTH-(1–31)-NH$_2$ (*[A^1,R^{19}]PTH(1–31)*) were replaced with Glu, and the effects on binding to the intact PTHR (*A* and *B*) and to PTHR-delNt (*C* and *D*) were assessed as described in the legend to Fig. 1. Data are the means ± S.E. of three or more experiments, each performed in duplicate. *^{125}I-PTH(1–34) SB*, ^{125}I-[Nle^{8,21},Tyr^{34}]rPTH-(1–34)-NH$_2$-specific binding.

reduced affinity for PTHR-delNt by ~4-fold ($p < 0.01$), similar to their effects on binding to the intact PTHR. The Arg^{19} → Glu substitution reduced affinity for PTHR-delNt by ~50-fold; this effect is consistent with the potency-enhancing effect seen for the reciprocal Glu^{19} → Arg substitution in PTH-(1–20) and PTH-(1–34) analogs in COS-7 cells expressing PTHR-delNt (24). The overall data obtained for these Glu substitutions support the view that the C-terminal domain of PTH-(1–31) interacts predominantly with the PTHR N domain, but can also contribute modestly to binding affinity via mechanisms that are independent of the N domain.

Analysis of Arg^{20}—The arginine at position 20 is one of the most conserved residues in PTH and PTHrP ligands and has been shown to play a key role in the receptor interaction process (10, 11, 25). Little has been revealed, however, about the mechanistic basis for this role. Barbier *et al.* (25) showed that none of 11 different amino acid analog substitutions at this position in PTH-(1–31)-NH$_2$ fully preserve cAMP-stimulating potency in ROS 17/2.8 cells. Thus, even the close arginine homologs of citrulline, (*S*)-4-piperidyl-(*N*-amidino)glycine (PipGly), and 4-piperidyl-(*N*-amidino)alanine reduce potency by 8-, 5-, and >21-fold, respectively, and lysine abolishes activity (25). To further dissect the functional role of Arg^{20}, we examined the same position 20-substituted PTH-(1–31)-NH$_2$ analogs from the study of Barbier *et al.* for the capacity to bind to the intact PTHR and to PTHR-delNt.

The replacement of Arg^{20} in PTH-(1–31)-NH$_2$ with Gln, Glu, Lys, (*S*)-2-amino-4-((2-amino)pyrimidinyl)butanoic acid (Apa), or L-(4-guanidino)phenylalanine (Gph) resulted in a complete loss of binding to the intact PTHR, and the substitutions with PipGly, Nle, and citrulline reduced affinity by ~200-fold relative to the parental peptide (Fig. 5, *A* and *B*; and Table 1). None of the position 20 substitutions altered binding to PTHR-delNt by >5-fold (Fig. 5, *C* and *D*; and Table 1). These results thus indicate that the effects of the substitutions at position 20 on binding to the PTHR are largely independent of interactions with the PTHR J domain.

Effects on cAMP and IP Signaling—Selected analogs of [Ala^1, Arg^{19}]PTH-(1–31)-NH$_2$ with Cha or Glu substitutions that markedly impaired binding to the intact PTHR were assessed for their capacity to stimulate cAMP production in ROS 17/2.8 cells. These cells endogenously express the rat PTHR at a moderate level (~70,000 PTHRs/cell) and were thus considered more useful for correlating effects on binding affinity and cAMP-signaling potency compared with HKRK-B7 cells, which express ~13-fold higher levels of receptor. Competition binding assays confirmed that the selected substitutions strongly impaired binding to ROS 17/2.8 cells and revealed effects on affinity that paralleled those seen in HKRK-B7 cells (Fig. 6*A* and Table 3). These effects on affinity in ROS 17/2.8 cell were accompanied by parallel reductions in cAMP-stimulating potency (Fig. 6*B* and Table 3). Although potency was reduced, each substituted analog (at the highest concentration) produced approximately the same maximum cAMP response as did the parental peptide.

We also assessed the alanine-substituted PTH-(1–31)-NH$_2$ analogs (at a single concentration of 1×10^{-6} M) for the capacity to stimulate IP production in COS-7 cells transfected with the PTHR. (ROS 17/2.8 and HKRK-B7 cells produce only barely detectable IP responses to PTH analogs.) In these assays, each analog produced the same ~4-fold increase in IP levels that was observed for the parental peptide (supplemental Fig. 2). Thus, the PTH-(1–31) analogs with C-terminal substitutions that strongly diminished PTHR-binding affinity could nevertheless mediate, at sufficiently high concentrations, robust cAMP- and IP-signaling responses. These findings are consistent with the notion that the principal ligand determinants of receptor activation, at least in terms of the $G\alpha_s$-mediated cAMP- and $G\alpha_q$-mediated IP_3-signaling responses, reside in the N-terminal portion of the ligand (19, 26) and are not directly perturbed by the tested substitutions in region 17–31.

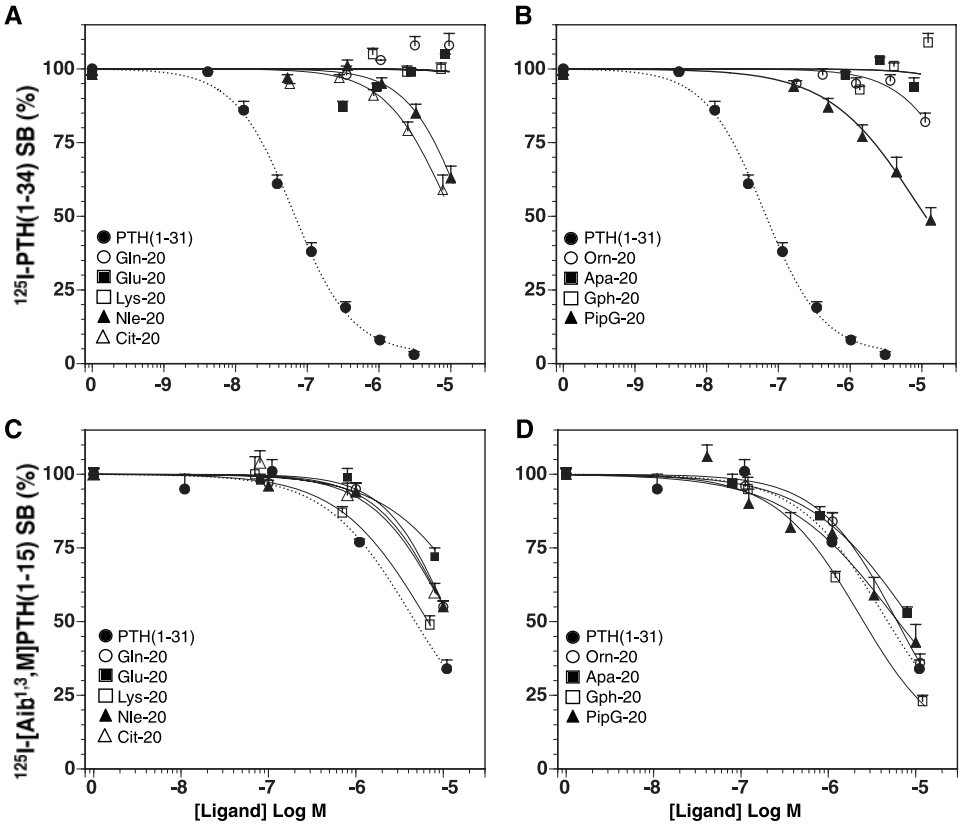

FIGURE 5. **Substitution analysis of Arg^{20}.** The effects of replacing the highly conserved arginine at position 20 of PTH-(1–31)-NH_2 with various encoded (Gln, Glu, and Lys) or non-encoded (Nle, citrulline (*Cit*), ornithine (*Orn*), Apa, Gph, and PipGly (*PipG*)) amino acids on binding to the intact PTHR (*A* and *B*) and to PTHR-delNt (*C* and *D*) were assessed by competition methods as described in the legend to Fig. 1. Data are the means ± S.E. of three or more experiments, each performed in duplicate. *^{125}I-PTH(1–34) SB*, ^{125}I-[Nle^{8,21},Tyr^{34}]rPTH-(1–34)-NH_2-specific binding.

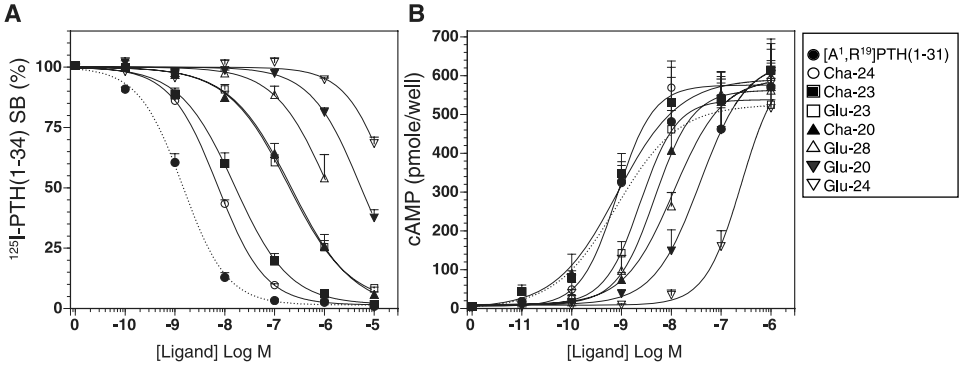

FIGURE 6. **Binding and cAMP-stimulating activities in ROS 17/2.8 cells.** The parental peptide [Ala^1,Arg^{19}]PTH-(1–31)-NH_2 (*[A^1,R^{19}]PTH(1–31)*) and Glu- or Cha-substituted analogs thereof were evaluated for the capacity to bind to the endogenous PTHR in ROS 17/2.8 cells (*A*) and to stimulate cAMP formation in these cells (*B*). Competition binding studies were performed in intact cells using ^{125}I-[Nle^{8,21},Tyr^{34}]rPTH-(1–34)-NH_2 (*^{125}I-PTH(1–34)*) as a tracer radioligand. Data are the means ± S.E. of data of three experiments, each performed in duplicate. *SB*, specific binding.

DISCUSSION

This study was designed to gain further information on the functional roles that the amino acid side chains in the principal receptor-binding domain of PTH play in the receptor interaction process. The experiments were based on the use of PTH-(1–31)-NH_2 or [Ala^1,Arg^{19}]PTH-(1–31)-NH_2 analogs containing a variety of substitutions in region 17–31 and the assessment of the effects of the substitutions on binding to the PTHR as well as to PTHR-delNt. Analysis of the binding of the analogs to PTHR-delNt expressed in COS-7 cell membranes was a key and novel aspect of our study, as it enabled us, for the first time, to assess the extent to which a targeted amino acid in the C-terminal domain of a relatively unmodified PTH ligand interacts with the receptor N domain (absent in PTHR-delNt) *versus* the receptor J domain containing the extracellular loops and transmembrane helices. Overall, our findings are largely consistent with the two-site model of the PTH-PTHR interaction mechanism outlined in the Introduction in that they suggest that the C-terminal domain of PTH-(1–31) interacts predominantly with the N domain of the receptor to contribute a large proportion of the overall binding energy to the complex. The data also suggest, however, that the C-terminal domain of the ligand can interact with the receptor J domain to gain a modest increase in the overall stability/affinity of the complex.

The greatest impact on the binding of our PTH-(1–31) peptides to the intact PTHR occurred with the non-conservative Glu substitutions at Arg^{20}, Trp^{23}, Leu^{24}, and Leu^{28}, as each reduced apparent affinity by 150-fold or more. Such effects are consistent with previous PTH substitution studies showing important roles for these four residues in binding to the intact PTHR (6, 9–11). The same Glu substitutions had little or no effect on binding to PTHR-delNt.

Our binding experiments performed with PTHR-delNt utilized membranes prepared from COS-7 cells that were cotransfected with PTHR-delNt and $G\alpha_s^{ND}$. (The negative-dominant $G\alpha_s$ mutant was utilized to improve the total binding of the ^{125}I-[Aib^{1,3},M]rPTH-(1–15)-NH_2 radioligand to the membrane preparations.) To assess the possibility that $G\alpha_s^{ND}$ *per se* could account for the lack of effect that the substitutions had on binding to PTHR-delNt, we performed control experiments in COS-7 cell membranes to evaluate the effects of several key substitutions (Cha^{20}, Glu^{20}, Glu^{23}, and Glu^{24}) on binding to the intact wild-type PTHR in the presence of $G\alpha_s^{ND}$. The experiments clearly showed that the substitutions again caused large decreases in binding affinity for the intact PTHR, even in the presence of $G\alpha_s^{ND}$ (supplemental Fig. 3).

TABLE 3

Activities in ROS 17/2.8 cells

[Ala^{1},Arg^{19}]PTH-(1–31)-NH$_2$ and analogs thereof containing the indicated substitutions were assessed in intact ROS 17/2.8 cells. Competition binding was assessed in intact cells using ^{125}I-[Nle^{8,21},Tyr^{34}]rPTH-(1–34)-NH$_2$ as a tracer radioligand. Values are the means ± S.E. of data from three experiments, each performed in duplicate.

	Binding IC_{50}	cAMP EC_{50}
	nM	
[Ala^{1},Arg^{19}]PTH-(1–31)-NH$_2$	1.6 ± 0.2	0.78 ± 0.24
Arg^{20} → Cha	290 ± 130	7.5 ± 3.0
Trp^{23} → Cha	19 ± 7	0.82 ± 0.11
Leu^{24} → Cha	7.3 ± 0.8	0.83 ± 0.17
Arg^{20} → Glu	5800 ± 1200	59 ± 31
Trp^{23} → Glu	220 ± 60	4.0 ± 2.0
Leu^{24} → Glu	29,000 ± 5000	250 ± 70
Leu^{28} → Glu	3100 ± 2100	11 ± 2

The lack of an effect of the substitutions on binding to PTHR-delNt must therefore be due to the absence of the receptor N domain and not to the presence of the $G\alpha_s^{ND}$ mutant.

Our CD analyses indicated that the substitutions did not cause major perturbations in the helical structure of the peptide. It thus seems clear from the data that the side chains of Arg^{20}, Trp^{23}, Leu^{24}, and Leu^{28} contribute to the PTHR-binding process by mechanisms that are largely, if not completely, dependent on interactions with the receptor N-terminal domain.

The side chains of Trp^{23}, Leu^{24}, and Leu^{28} form the hydrophobic face of the amphiphilic α-helix predicted to reside within region 17–31 of PTH (6, 7). Our data predict that this hydrophobic helical face contributes to the PTHR-binding process by interacting with the N-terminal domain of the receptor. Our findings do not support a mechanism by which this hydrophobic face contributes to the PTHR-binding process by interacting nonspecifically with the lipid component of the cell membrane, as has been discussed for PTH (32) and for amphiphilic peptide ligands in general (33). If this were the case, then the substitutions would have impacted equally the binding of the ligand to the intact PTHR and to PTHR-delNt, which did not occur. Moreover, the hydrophobic Cha substitutions at Trp^{23} and Leu^{24} reduced binding to the intact PTHR by ~12-fold and again had little or no effect on binding to PTHR-delNt (Table 2). Thus, the mechanisms by which the side chains of Try^{23} and Leu^{24} contribute to the PTHR-binding process are not likely to be based simply on nonspecific hydrophobic interactions with the lipid bilayer, but instead involve additional spatial and chemical features of the side chains and their specific interactions with cognate functional groups in the receptor.

It is clear from our data and that presented elsewhere (10, 11, 25) that Arg^{20} of PTH plays a key role in the PTHR-binding process. Each of 10 substitutions tested at this position in PTH-(1–31)-NH$_2$ reduced affinity for the intact PTHR by at least ~200-fold, and most (seven) abolished detectable binding. Each of these substitutions had only a minor effect on binding to PTHR-delNt. The side chain of Arg^{20}, like those of Trp^{23}, Leu^{24}, and Leu^{28}, must therefore contribute to the PTHR-binding process via a mechanism that primarily involves interactions with the PTHR N domain. The molecular nature of these interactions is not clear at present, but likely involves multiple components of the arginine side chain, including the cationic and H-bonding nitrogen atoms of the guanidino group and the three methylenes of the linker (25). Our data now imply that these functional groups of the Arg^{20} side chain fit within a highly specific binding pocket within the N domain of the receptor.

Unlike Arg^{20}, residue 19 of PTH appears to interact predominantly with the PTHR J domain (24). This can be seen in our present data by the 90-fold reduction in binding affinity for PTHR-delNt caused by the Arg^{19} → Glu substitution, the strongest effect on binding to PTHR-delNt of any substitution in this study. This reduction in binding affinity mirrors the enhancing effect that the Glu^{19} → Arg substitution in either PTH-(1–34) or PTH-(1–20) analogs has on cAMP-stimulating potency in COS-7 cells expressing PTHR-delNt (24). That residue 19 of the bound ligand is in spatial proximity to the PTHR J domain is further suggested by the cross-linking of Bpa^{19}-containing PTH analogs to the extracellular end of transmembrane helix 2 of the PTHR (34). When considered together, the data for residues 19 and 20 suggest that the 19/20-position in the ligand marks a point of divergence for the ligand segments that interact predominantly with the N and J domains of the receptor: regions 20–31 and 1–19 of PTH, respectively.

We observed subtle but consistent effects of substitutions at positions 21 and 25–27 in our PTH-(1–31) peptides on interaction with PTHR-delNt. These effects were accompanied by approximately proportional effects on interaction with the intact PTHR. Such findings suggest that the side chains of these residues, although not making major contributions to overall binding energy, can promote binding via mechanisms that involve interactions with the PTHR J domain. The cationic side chains of Arg^{25}, Lys^{26}, and Lys^{27} form the hydrophilic face of the predicted amphiphilic α-helix in the C-terminal domain of the ligand, and Val^{21} lies at the edge of this face (8). It is possible that the side chains projecting from this helical face contribute to binding indirectly, for example, by interacting with the phospholipid head group and/or aliphatic components of the cell membrane (32, 33), as discussed above. Another possibility is that these side chains interact with anionic and/or hydrophobic groups in the extracellular loops and/or transmembrane domain regions of the receptor. The cross-linking of [Lys^{27}(Bp)$_2$]PTH-(1–34)-NH$_2$ to the first extracellular loop of the PTHR indeed suggests a physical proximity of this helical face in the ligand and the PTHR J domain (23). The possibility for a modest functional interaction between the C-terminal helix and the PTHR J domain is also supported by our recent finding that backbone methylations at Ser^{17}, Trp^{23}, and Lys^{26} in PTH-(1–31)-NH$_2$ impair the capacity of the ligand to stimulate cAMP production via PTHR-delNt (8).

If both the C-terminal (region 20–31) and N-terminal (region 1–19) domains of the ligand interact with the PTHR J domain, then a bend would most likely be required between the two domains of the receptor-bound ligand. The tertiary structure of receptor-bound PTH has been a matter of some debate, with linear and folded structures supported (4, 35). A folded helix-turn-helix structure for PTH-(1–34) was indeed pre-

dicted early on based on modeling and structure-activity data (36), and solution-phase NMR studies of PTH and PTHrP ligands generally reveal mid-region flexibility or a hinge between the N- and C-terminal domains (4, 5, 37, 38). A bend in receptor-bound PTH-(1–34) has more recently been suggested by the cross-linking of both [Bpa^{11}]PTH-(1–34) and [Bpa^{21}]PTH-(1–34) to the same segment (Ala^{165}–Asn^{176}) of the PTHR N domain (39).

In addition to the tertiary structure of the bound ligand, our data have implications for the topology of the occupied receptor and the spatial relationship of the N and J domains. If the C-terminal α-helical domain (region 20–31) of PTH interacts with both the N and J domains of the receptor via its hydrophobic and hydrophilic faces, respectively, as supported by this study, then the N and J domain-binding sites in the receptor must be near each other. This possibility is again supported by cross-linking data: specifically, the cross-linking of one PTH-(1–34) analog with a photolabile Bp moiety incorporated at position 27 as a Bpa substitution with the receptor N domain (22) and that of another PTH-(1–34) analog with the Bp moiety attached to the distal amino groups of the Lys^{27} side chain with the first extracellular loop of the receptor (23). Because the spatial positioning of the Bp moieties in these two ligands is likely to be similar, a proximity of the two cross-linked sites in the receptor is also likely.

The available data derived from the functional and cross-linking studies combined thus suggest some intriguing hypotheses regarding the topology and domain architecture of the PTH·PTHR complex. However, the lack of direct structural information on receptor-bound PTH or on the intact PTHR itself hampers our capacity to assimilate such data into a detailed three-dimensional model of the PTH·PTHR complex. One important goal that may be facilitated by our work is to identify sites in the receptor that are used by key ligand residues such as Arg^{20}, Trp^{23}, Leu^{24}, and Leu^{28}. Our results predict that such interaction sites will be located in the receptor N-terminal domain. For Trp^{23}, the extreme N-terminal segment (Thr^{33}–Leu^{40}) of the N domain needs to be considered, as it contains the cross-linking site for [Bpa^{23}]PTHrP-(1–36) (34). For the other ligand residues, few clues are available: cross-linking has not been achieved for positions 20 and 24, and [Bpa^{28}]PTHrP-(1–36) cross-links to a nonessential segment (Ser^{61}–Gly^{105}) of the N-terminal domain (34).

The recently reported NMR-derived structure of the N-terminal domain of the related corticotropin-releasing factor receptor (15) may open paths for structure-based analyses of the ligand interaction sites in the N domains of the Class 2 G protein-coupled receptors (14). Even with such an approach, additional functional studies will be needed. The new PTH analogs presented here should be of value in this regard, as they can be used in conjunction with PTHR mutants altered at candidate sites in the N-terminal domain to probe for allele-specific rescue effects. This is a direction that we hope to pursue in future studies.

Acknowledgments—We thank Dr. John T. Potts, Jr., for careful review of the manuscript and Dr. Catherine Berlot for kindly providing the plasmid encoding $G\alpha_s^{ND}$.

REFERENCES

1. Strewler, G. J. (2000) *N. Engl. J. Med.* **342,** 177–185
2. Tregear, G. W., Van Rietschoten, J., Greene, E., Keutmann, H. T., Niall, H. D., Reit, B., Parsons, J. A., and Potts, J. T., Jr. (1973) *Endocrinology* **93,** 1349–1353
3. Nussbaum, S. R., Rosenblatt, M., and Potts, J. T., Jr. (1980) *J. Biol. Chem.* **255,** 10183–10187
4. Pellegrini, M., Royo, M., Rosenblatt, M., Chorev, M., and Mierke, D. F. (1998) *J. Biol. Chem.* **273,** 10420–10427
5. Chen, Z., Xu, P., Barbier, J.-R., Willick, G., and Ni, F. (2000) *Biochemistry* **39,** 12766–12777
6. Neugebauer, W., Surewicz, W. K., Gordon, H. L., Somorjai, R. L., Sung, W., and Willick, G. E. (1992) *Biochemistry* **31,** 2056–2063
7. Epand, R. E. (1983) *Mol. Cell. Biol.* **57,** 41–47
8. Barbier, J.-R., Gardella, T. J., Dean, T., MacLean, S., Potetinova, Z., Whitfield, J. F., and Willick, G. E. (2005) *J. Biol. Chem.* **280,** 23771–23777
9. Gardella, T. J., Wilson, A. K., Keutmann, H. T., Oberstein, R., Potts, J. T., Jr., Kronenberg, H. M., and Nussbaum, S. R. (1993) *Endocrinology* **132,** 2024–2030
10. Oldenburg, K. R., Epand, R. F., D'Orfani, A., Vo, K., Selick, H., and Epand, R. M. (1996) *J. Biol. Chem.* **271,** 17582–17591
11. Reidhaar-Olson, J., Davis, R., De Souza-Hart, J., and Selick, H. (2000) *Mol. Cell. Endocrinol.* **160,** 135–147
12. Gensure, R. C., Gardella, T. J., and Jüppner, H. (2005) *Biochem. Biophys. Res. Commun.* **328,** 666–678
13. Hoare, S. R. J., Gardella, T. J., and Usdin, T. B. (2001) *J. Biol. Chem.* **276,** 7741–7753
14. Tan, Y. V., Couvineau, A., Murail, S., Ceraudo, E., Neumann, J. M., Lacapere, J. J., and Laburthe, M. (2006) *J. Biol. Chem.* **281,** 12792–12798
15. Grace, C. R., Perrin, M. H., DiGruccio, M. R., Miller, C. L., Rivier, J. E., Vale, W. W., and Riek, R. (2004) *Proc. Natl. Acad. Sci. U. S. A.* **101,** 12836–12841
16. Dong, M., Pinon, D. I., and Miller, L. J. (2005) *Mol. Endocrinol.* **19,** 1821–1836
17. Luck, M. D., Carter, P. H., and Gardella, T. J. (1999) *Mol. Endocrinol.* **13,** 670–680
18. Dean, T., Linglart, A., Mahon, M. J., Bastepe, M., Jüppner, H., Potts, J. T., Jr., and Gardella, T. J. (2006) *Mol. Endocrinol.* **20,** 931–942
19. Shimizu, M., Potts, J. T., Jr., and Gardella, T. J. (2000) *J. Biol. Chem.* **275,** 21836–21843
20. Shimizu, N., Guo, J., and Gardella, T. J. (2001) *J. Biol. Chem.* **276,** 49003–49012
21. Mannstadt, M., Luck, M. D., Gardella, T. J., and Jüppner, H. (1998) *J. Biol. Chem.* **273,** 16890–16896
22. Gensure, R. C., Gardella, T. J., and Jüppner, H. (2001) *J. Biol. Chem.* **276,** 28650–28658
23. Greenberg, Z., Bisello, A., Mierke, D. F., Rosenblatt, M., and Chorev, M. (2000) *Biochemistry* **39,** 8142–8152
24. Shimizu, M., Shimizu, N., Tsang, J. C., Petroni, B. D., Khatri, A., Potts, J. T., Jr., and Gardella, T. J. (2002) *Biochemistry* **41,** 13224–13233
25. Barbier, J.-R., MacLean, S., Whitfield, J. F., Morley, P., and Willick, G. E. (2001) *Biochemistry* **40**, 8955–8961
26. Takasu, H., Guo, J., and Bringhurst, F. (1999) *J. Bone Miner. Res.* **14,** 11–20
27. Yamamoto, I., Shigeno, C., Potts, J. T., Jr., and Segre, G. V. (1988) *Endocrinology* **122,** 1208–1217
28. Shimizu, M., Carter, P. H., Khatri, A., Potts, J. T., Jr., and Gardella, T. J. (2001) *Endocrinology* **142,** 3068–3074
29. Berlot, C. H. (2002) *J. Biol. Chem.* **277,** 21080–21085
30. Shimizu, N., Dean, T., Tsang, J. C., Khatri, A., Potts, J. T., Jr., and Gardella, T. J. (2005) *J. Biol. Chem.* **280,** 1797–1807
31. Chakrabartty, A., Schellman, J. A., and Baldwin, R. L. (1991) *Nature* **351,** 586–588
32. Pellegrini, M., Bisello, A., Rosenblatt, M., Chorev, M., and Mierke, D. F. (1998) *Biochemistry* **37,** 12737–12743
33. Sargent, D., and Schwyzer, R. (1986) *Proc. Natl. Acad. Sci. U. S. A.* **83,**

5774–5778
34. Gensure, R. C., Shimizu, N., Tsang, J. C., and Gardella, T. J. (2003) *Mol. Endocrinol.* **17,** 2647–2658
35. Jin, L., Briggs, S. L., Chandrasekhar, S., Chirgadze, N. Y., Clawson, D. K., Schevitz, R. W., Smiley, D. L., Tashjian, A. H., and Zhang, F. (2000) *J. Biol. Chem.* **275,** 27238–27244
36. Cohen, A. E., Strewler, G. J., Bradley, M. S., Carlquist, M., Nilsson, M., Ericsson, M., Ciardelli, T. L., and Nissenson, R. A. (1991) *J. Biol. Chem.* **266,** 1997–2004
37. Barden, J. A., and Kemp, B. E. (1994) *Biochim. Biophys. Acta* **1208,** 256–262
38. Peggion, E., Mammi, S., Schievano, E., Silvestri, L., Schiebler, L., Bisello, A., Rosenblatt, M., and Chorev, M. (2002) *Biochemistry* **41,** 8162–8175
39. Wittelsberger, A., Corich, M., Thomas, B. E., Lee, B. K., Barazza, A., Czodrowski, P., Mierke, D. F., Chorev, M., and Rosenblatt, M. (2006) *Biochemistry* **45,** 2027–2034

Role of Amino Acid Side Chains in Region 17–31 of Parathyroid Hormone (PTH) in Binding to the PTH Receptor

Thomas Dean, Ashok Khatri, Zhanna Potetinova, Gordon E. Willick and Thomas J. Gardella

J. Biol. Chem. 2006, 281:32485-32495.
doi: 10.1074/jbc.M606179200 originally published online August 21, 2006
